Brittle deformation history of fault rocks on the Fosen Peninsula, Trøndelag, Central Norway

ARNE GRØNLIE, BJØRN NILSEN & DAVID ROBERTS

Grønlie, A., Nilsen, B. & Roberts, D. 1991: Brittle deformation history of fault rocks on the Fosen Peninsula, Trøndelag, Central Norway. *Nor.geol.unders.Bull.421,* 39-57.

Late- and post-Caledonian fault deformation of rock units on the Fosen Peninsula follows a time sequence wherein lower crustal ductile deformation was followed by several episodes of brittle fragmentation, some with coeval hydrothermal mineral precipitation. Field evidence, including various minor structures and hydrothermal parageneses, supported by fission-track and palaeomagnetic dating, indicates the following general history of development: (1) Sinistral ductile shear in Early to Middle Devonian times is manifested both in regional southwest-directed shear and in concentrated strike-slip movement along the Verran Fault. (2) A phase of retrogression of the mylonitic rocks can be recognised within and close to the principal displacement zones. (3) Several episodes of brittle faulting followed, some of which were accompanied by major pulses of hydrothermal fluid penetration. Principal brittle faulting events occurred in Late Devonian, Permo-Triassic and post- Mid-Jurassic times. A major phase of zeolite fault mineralisation was associated with the post- Mid-Jurassic event. (4) Dip-slip normal faulting along the MTFZ characterised the Late Jurassic/Early Cretaceous period but was directly followed by a component of dextral strike-slip movement. (5) NW-SE trending extensional joints and subordinate faults in the Outer Fosen district are considered to relate mainly to Tertiary tectonic events and in particular to a stress field created by ridge-push forces generated from the Mid-Atlantic spreading ridge. (6) NW-SE to NNW-SSE minor joints with plumose and fringe structures represent a latest stage of brittle fracturing on the Fosen Peninsula; these mesojoints may have been initiated in post-glacial times.

Arne Grønlie & David Roberts, Norges geologiske undersøkelse, Postboks 3006-Lade, N-7002 Trondheim, Norway.
Bjørn Nilsen, Institutt for Geologi og Bergteknikk, Norges Tekniske Høgskole, N-7034 Trondheim-NTH, Norway.

Introduction

In an earlier study of the northeastern part of the Møre-Trøndelag Fault Zone (MTFZ) (Gabrielsen & Ramberg 1979a, 1979b, Gabrielsen et al. 1984) northwest of Trondheimsfjord, analysis was based largely on an integration of satellite imagery, aerial photographs and existing geological maps (Grønlie & Roberts 1989). This showed an array of faults and fractures reflecting a geometric arrangement akin to that of a major dextral strike-slip fault zone. It was emphasised, however that the MTFZ had existed as a zone of major crustal weakness since at least the time of the Caledonian orogeny, and that slip motions have varied appreciably, from strike-slip to dip-slip, at different points in time.

In the present account we compare and discuss the nature of brittle fracturing and fault rock products in two selected areas on the Fosen Peninsula, one within and the other outside the MTFZ. Verrabotn-Beitstadfjord, located within the MTFZ, was chosen because the bedrock there shows abundant brittle deformation structures along the main fault zones. As the fault rocks developed both below and above the brittle/ductile transition (Sibson 1977) and also carry upper crustal zeolite mineralisation, a relative timing of events can be established.

The second area is situated on the coast, near Stokksund, and is dominated by NW-SE trending fractures. Field mapping has shown that these fractures are mostly vertical extension joints and their consistent occurrence over the entire Outer Fosen coastal region would seem to indicate that this particular trend is of more than local significance.

Comparison of the fault and fracture patterns in these two areas shows easily noticeable disparate trends, which epitomises the contrasting lineament patterns seen in the Outer and Inner Fosen districts, to the north and to the south of the Hitra-Snåsa Fault, respectively (Fig. 1a-c).

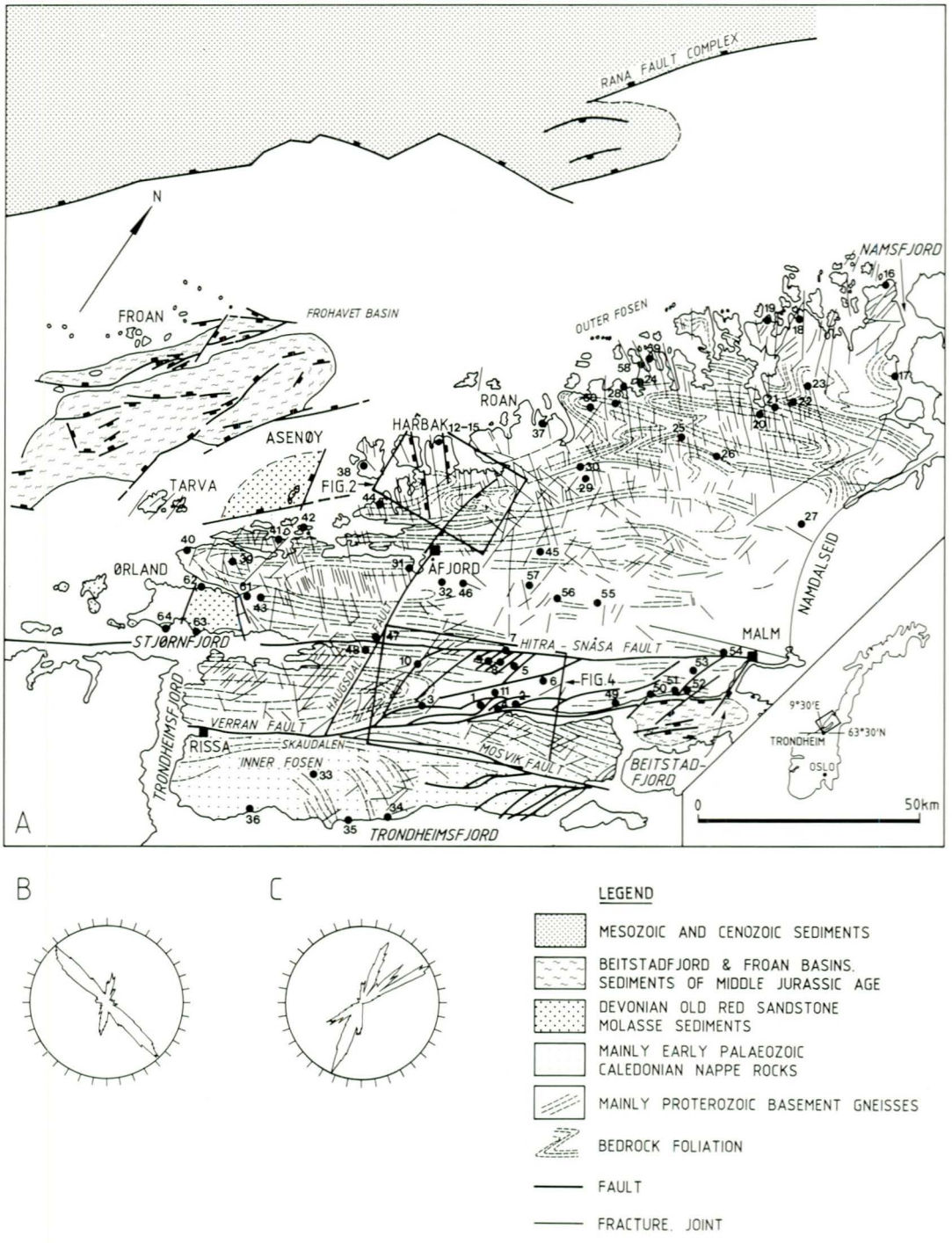

Fig. 1 (A): Simplified bedrock geology and tectonic map of the Fosen Peninsula, Central Norway, showing the main geological units and faults as well as foliation trends. (b): TM-lineament trends in the crystalline basement of the Outer Fosen area, northwest of the Hitra-Snåsa Fault. Number of lineaments = 397. (c): TM-lineament trends of the Inner Fosen area, southeast of the Hitra-Snåsa Fault. Number of lineaments = 87. The numbers show locations for measurement of fracture populations (cf. rose diagrams in Fig. 3, 1-64). Offshore fault interpretations from Bøe (pers.comm.1989) (Frohavet), Bøe & Bjerkli (1989) (Beitstadfjord) and Bøe & Sturt (1991) (Asenøy area).

Geological setting

The bedrock of the Fosen Peninsula, north of the prominent Verran Fault (Fig.1a) is dominated by heterogeneous, Proterozoic migmatitic banded gneisses (Wolff 1976, Gee et al. 1985, Solli 1990). The gneisses are tectonostratigraphically overlain by amphibolite-facies psammites, schists and amphibolites, and higher up by low-grade metasediments and greenstones. These 'cover' rocks represent slices of the Lower, Middle and Upper Allochthons of the Caledonide orogen (Gee et al.1985). The Proterozoic gneissic rocks are also strongly banded and Caledonised and are considered to form part of the Lower Allochthon. South of the Verran Fault, the bedrock consists mainly of Caledonian nappe rocks of the Upper Allochthon (Thorsnes & Grønlie 1990).

On Ørland and in the Asenøy area (Fig.1a), Late Silurian to Middle Devonian, Old Red Sandstone molasse sediments are present (Siedlecka 1975, Bøe & Sturt 1991). In the Verran area the geology of Beitstadfjord provides evidence bearing on the age of fault movements along the MTFZ. Fragments of coal and pebbles of sideritic ironstone with plant fossils found along the shores of this fjord are believed to have been derived from the fjord bottom (Horn 1931, Oftedahl 1975) and are of Middle Jurassic age. A recent shallow-seismic profiling survey has largely confirmed Oftedahl's original Beitstadfjord interpretation and has also provided additional information on the Late to post-Mesozoic fault pattern (Bøe & Bjerkli 1989). This shows that the Jurassic rocks are preserved in a half-graben structure whose main (Verran) fault strikes NE-SW close to the northern Beitstadfjord shoreline. The Fosdalen Fault trend, NNE-SSW, is also an important element of the Beitstadfjord structural framework (Bøe & Bjerkli 1989).

Stokksund area

The coastal district of Stokksund and Skjørafjorden is dominated by a set of vertical fractures trending N40°W (Figs.2a & b). Bedrock mapping (Grønlie & Möller 1988, Fossen et al. 1988) has shown that the Landsat-TM and photolineaments of this area are, in fact, mainly extensional joints and faults, the former being dominant.

In the field, most map-scale fractures show up as vertical joints with walls typically 5-10m apart. The fractures are generally remarkably straight for several kilometres along strike (Fig.2a), and splays or en echelon patterns are not common. The proven faults, the Harbak, Stokkøy and Bjørnahovud faults, show evidence of normal dip-slip movement. Mylonitic and brecciated rocks testifying to a prolonged history of faulting have been found only along the Stokkøy fault. On account of the commonly homogeneous nature of the gneissic lithology, faults could only be defined by detailed bedrock mapping and even then the amount of throw on individual faults is uncertain. In the absence of fault rock products it is generally not possible to distinguish between master joints and faults due to a lack of marker horizons.

Depending on lithology, mesoscopic joints are in places bordered by thin, red, hydrothermal alteration haloes, generally extending 0.5-1cm on either side of the central joint. This is a conspicuous feature of the Harbak Peninsula (Fig.2a) where thin, NW-SE trending veins transect the granitic migmatite gneiss. The overlying garnet amphibolite is dissected by ubiquitous thin joints of the same trend, but without the red alteration.

Regional significance of the NW-SE trend

Fracture populations have been measured on outcrop at 64 different localities on the Fosen Peninsula, providing good geographical coverage of the study area (Fig.3, *1-64*). A total of ca. 2,400 joint orientations were measured. The strikes and dips of ca. 40 randomly recorded joints were measured at each locality. The vast majority of dips are in the 80-90° range, and joint orientations are thus conveniently illustrated by rose diagrams. The NW-SE to NNW-SSE fracture trend is a dominant one in approximately 40 of the measured sites, and this trend is also most pronounced north of the MTFZ. However, the nature of fracturing on this scale is much more heterogeneous than that shown by the map-scale features, the meso-fractures being more influenced by local stress field variations.

The average length of NW-SE trending lineaments north of the Hitra-Snåsa Fault (HSF) between Ørland and Namsfjorden, as measu-

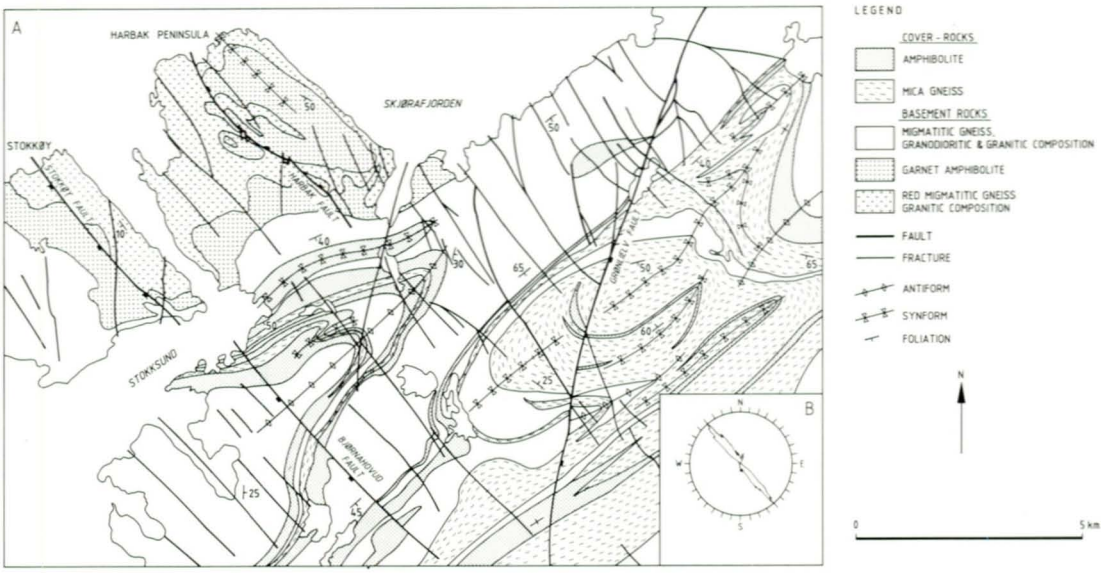

Fig. 2 (a): Simplified geological map of the Stokksund area (Grønlie & Möller 1988, Fossen et al. 1988). (b): Rose diagram of joints and faults occurring in the area of Fig. 2a. Number of fractures = 84.

red from the TM-lineament interpretation (Fig. 1a), is 3.1 km. The average fracture spacing is 1.1 km. For lineaments longer than 1 km, air-photo and TM-lineament interpretations are almost identical (Rindstad & Grønlie 1987). Concerning fracture depth, Gudmundsson (1987) stated that in evolving tension-crack systems, crack depth should be of the same order of magnitude, or less, than crack spacing, thus indicating a shallow upper crustal development for most of these fractures.

As indicated by the lineament interpretation and later confirmed by bedrock mapping, the NW-SE trending fracture set is well developed northwest of the Haugsdal and Grønlielv faults (Fig.1a, 2a) even though identical lithological units are present on either side of these faults. Also, the abundance of these fractures generally decreases with distance from the coastline. Pleistocene glacial erosion would have tended to emphasize fractures of this trend as they are oriented parallel to the direction of principal ice movement during the glaciations (Reite 1987). Field mapping has confirmed that the decreasing fracture frequency on a coast to inland profile is real. Within the MTFZ on Fosen, larger fractures of this trend are less prominent (Fig.1c), but the trend is nevertheless significant on a meso-scale along the Verran and Hitra-Snåsa (Faults (Fig.3-4).

Bøe & Bjerkli (1989) noticed that the NW-SE fracture trend is a major one in the Mesozoic rocks of the coastal Edøyfjord basin, while apparently being absent in the inland Beitstadfjord basin. In the Devonian rocks of Ørlandet, Siedlecka (1975) found two main fracture sets, NW-SE and NE-SW, post-dating the Late Devonian Svalbardian fold structures.

Aanstad et al. (1981) found four statistically important fracture trends to prevail in the Møre-Trøndelag region; the bimodal ENE-WSW and NE-SW (MTFZ) trend, as well as N-S and NW-SE to NNW-SSE trends. Mesozoic brittle deformation was claimed for the MTFZ trends as well as for the NW-SE to NNW-SSE trend. It was noted by Aanstad et al. (1981) that the N-S trend is parallel to what they termed the Oslo-Trondheim and Bergen Zones, characterised by possible Permian movements. A high degree of correlation between onshore and offshore data was evident and showed basement-imposed control on the structural pattern offshore.

Verrabotn - Beitstadfjord area

In this area (Fig.4a) the Verran Fault forms a prominent topographic lineament running along Skaudalen from Rissa to Verrasundet. Further to the east-northeast it forms the northern

bounding fault of the Beitstadfjord half-graben (Bøe & Bjerkli 1989). The Verran Fault, together with its subsidiary faults, the Elvdal, Rautingdal and Skurven faults, constitute the Verran Fault System (VFS).

The VFS displays a variety of fault rocks belonging to the brittle or elasto-frictional regime of Sibson (1977). The brittle fault rocks include fault breccias, cataclasites, pseudotachylyte and mineral-filled extensional veins. The various brittle fault rocks occur centrally in all main lineaments such as the Verran, Elvdal, Rautingdal and Skurven faults (Fig.4a).

Although this paper is concerned principally with describing brittle deformation, it is appropriate to comment briefly on aspects of the pre-Mesozoic ductile deformation along the Verran Fault. In the Verrabotn area, the Verran Fault defines a 0.5-1 km wide, ductile shear zone, in which regional-scale foliation trajectories are seen to be drawn into the high-strain zone. The fault rocks of this ductile deformation zone include most of the mylonite series rocks as defined by Sibson (1977), as well as augen gneiss and a protomylonitic porphyry granite of possible Caledonian age. Kinematic indicators, which include asymmetric feldspar augen, displaced broken feldspar porphyroclasts and S-C structures mostly indicate sinistral movement along the shear zone. The

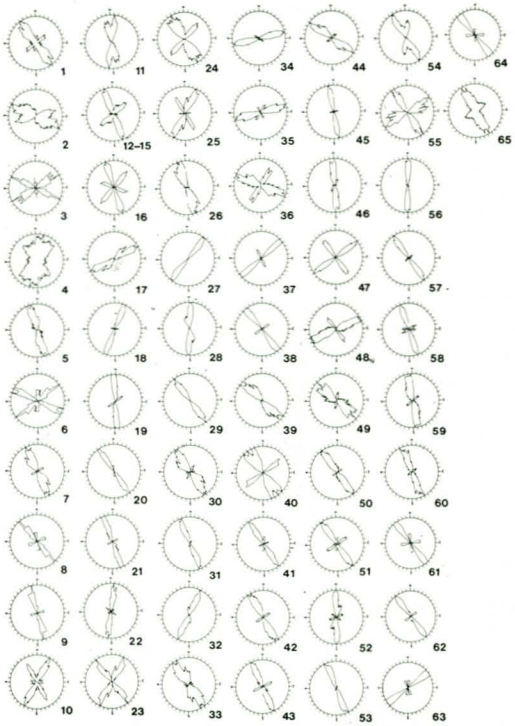

Fig. 3: Rose diagrams of 64 fracture populations measured on outcrop. Each location represents ca. 40 fractures. The position of each location is shown in Fig.1a. No. 65 represents a rose diagram of the total number of measured fractures (N=2,400).

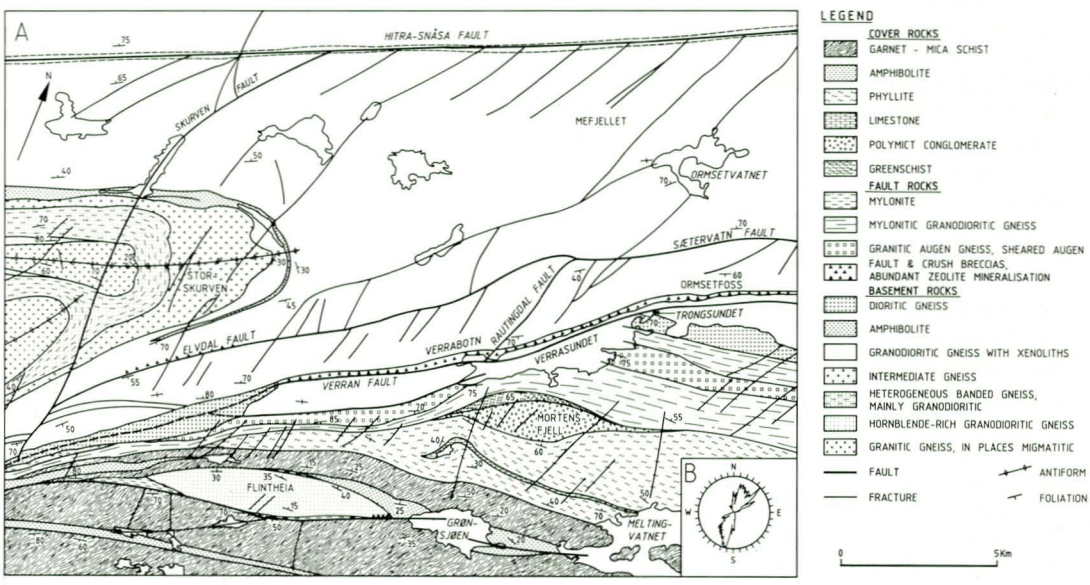

Fig. 4 (a): Simplified geological map of the Verrabotn area. (b): Rose diagram of faults and joints occurring in the area of Fig. 4a. Number of fractures = 110.

mylonites show a stretching lineation defined by elongate quartz and feldspar grains, in general plunging at 20° towards the northeast, a lineation which is considered to reflect the shear movement. The mylonites, derived from a granodiorite protolith, are commonly strongly retrograded. They show chloritisation of biotite, as well as albitisation, adularisation and epidotisation of plagioclase. Primary, strained quartz in quartz ribbons shows evidence of replacement by unstrained quartz grains.

The possibility exists that the mylonites and shear zones are related to one or more episodes of Late- to post-Caledonian, sinistral, strike-slip or oblique-slip, shear movement and not to regional overthrusting of the nappe rocks. Piasecki & Cliff (1988) proposed that this region was affected by a major Early to Middle Devonian (ca.389 Ma) episode of orogen-parallel ductile shear with top-to-the-southwest movement. The ductile structures in the Verrabotn area would seem to support this view.

To the north, the Hitra-Snåsa Fault and its subsidiary faults (Fig.1a & 4a) show similar mylonites but the brittle overprint is less pronounced than along the VFS, although fine examples of quartz-epidote rich breccias and pseudotachylyte occur (Fig.7e & f). The common minerals of the brittle fault rocks here are quartz, epidote and minor calcite, and there is no late zeolite mineralisation.

The Verran Fault

Along the Verran Fault a cataclasite (VB1) is commonly present, overprinting the retrograde mylonite. The cataclasite usually consists of subrounded to subangular, medium-sized fragments of retrograded mylonite, albitised plagioclase, secondary epidote and calcite in a matrix of epidote, albite, K-feldspar and finely comminuted mylonite (Fig. 5d). Prehnite, chlorite and calcite also occur, although less commonly, as matrix minerals. The cataclastic rock generally consists of irregular zones of deformed material which anastomose between lenses of less deformed, retrograded mylonite. In places, thin ultracataclasite stringers transect this fault rock. A similar cataclasite (RB1) occurs along the Rautingdal fault (Fig. 5a-c).

The character of the fragments of the VB1 cataclasite, subangular to subrounded, points to a prolonged period of faulting with milling and grinding of the fragments or fluidisation. Torske (1983) has maintained that a fluid consisting of CO_2 and H_2O would induce a high solubility for anorthite as compared to albite and K-feldspar and this is consistent with deposition of Ca-minerals upon loss of CO_2, leading to rapid deposition of epidote and probably calcite. It has been shown by Sibson et al. (1975) and Sibson (1987) that significant amounts of hydrothermal fluids migrate upwards through fault zones by the mechanism of seismic pumping following major earthquake movements. This is also manifested in the local abundance of hydrothermally cemented, high-dilation, wall-rock breccias showing multiple brecciation.

Evidence of abundant, early, distributed cracking (Sibson 1986) of the Verran and Rautingdal mylonites is widespread as shown by epidote-mineralised micro-faults (Fig. 5e) and minor shear zones (Fig. 5f).

A common rock-type along the Verran Fault, trending parallel to the principal deformation zone, is a greyish-green crush breccia (VB2) (Fig. 6a) which consists mainly of angular, coarse-grained fragments of retrograded mylonite in a fine- to medium-grained matrix. Plagioclase in the mylonite fragments is always heavily saussuritised and shows a high content of epidote, and biotite is altered to chlorite. Rare fragments of vein prehnite also occur. In addition, the breccia contains vein epidote fragments as well as composite clasts, which testify to at least two earlier episodes of brecciation or several stages of the same ongoing brecciation. Some of these contain pseudotachylyte and thus point to an early deformation achieved by dry, seismic slip (Sibson 1975). The main matrix minerals are quartz and epidote, but comminuted mylonite is also present. The matrix quartz is unstrained. The VB2 breccia is cut by 1-2 mm wide ultracataclasites with a quartz matrix and by epidote veinlets. It is also transected by abundant late, micro- and meso-faults, as well as joints. The process of formation is considered to have been attrition brecciation (Sibson 1986).

Along the Verran Fault both mylonites and crush breccias are cut by prehnite-matrix breccias (VB3) that show a pronounced NNE-SSW trend, which happens to be parallel to the Rautingdal Fault (Fig. 4a). These breccias, which are generally 1-10 cm in thickness, display rotated and angular fragments of mylonite. The matrix consists mainly of prehnite and opaline quartz, but minute fragments of mylon-

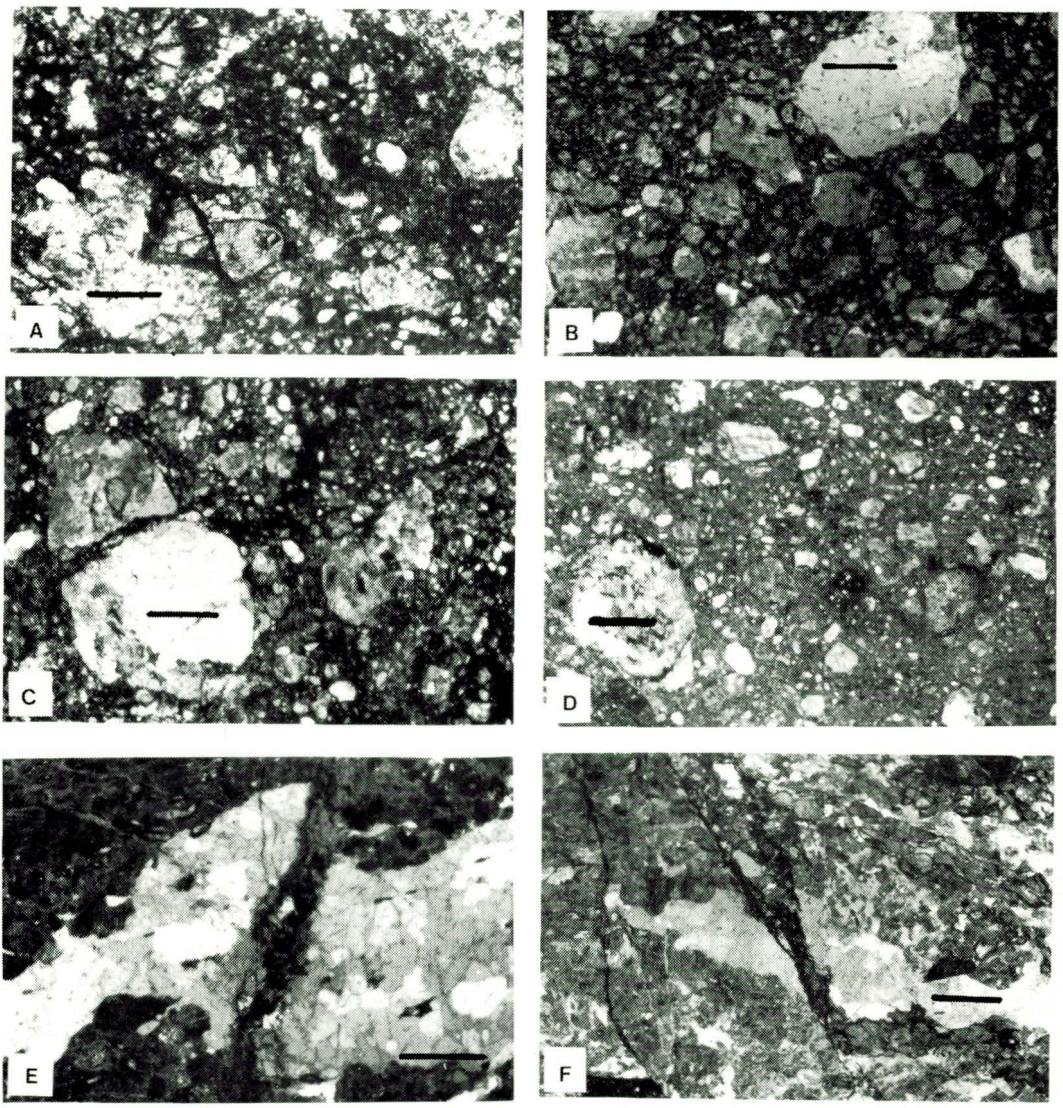

Fig. 5: VFS cataclasites.
a) Rautingdal fault, sample R1 (579.15 7077.15). RB1 cataclasite. Subrounded fragments of retrograded mylonite and epidote in fine-grained matrix. Note microfaulted sphene grain. Scale bar is 0.5mm.
b) Rautingdal fault, sample 347 (579.30 7077.60). RB1 cataclasite. Subangular to subrounded fragments of albite, epidote and retrograded mylonite in a finely comminuted matrix of the same minerals. Scale bar is 0.5mm.
c) Rautingdal fault, sample VA 11b (579.10 7077.15). RB1 cataclasite. Subangular to subrounded fragments of albite, epidote and retrograded mylonite in a finely comminuted matrix of the same minerals. Scale bar is 0.5mm.
d) Verran Fault, sample VA40 (580.50 7078.30). VB1 cataclasite. Subrounded fragments of albite and retrograded mylonite, as well as calcite, in a fine-grained matrix of the same minerals. Scale bar is 0.5mm.
e) Rautingdal fault, sample 346 (579.22 7077.40). Microfaulted quartz-ribbon in mylonitic granodiorite. The fracture is epidote filled. Scale bar is 0.25mm.
f) Verran Fault, sample 89-858-5 (581.70 7079.70). Microfaulted quartz-ribbon in retrograded mylonite. Scale bar is 0.5mm.

ite are also common. The contact towards mylonite is commonly marked by well defined slickensided fault planes mostly documenting dip-slip movement. The mechanism of formation was probably that of implosion brecciation (Sibson 1986). These high-dilation breccias

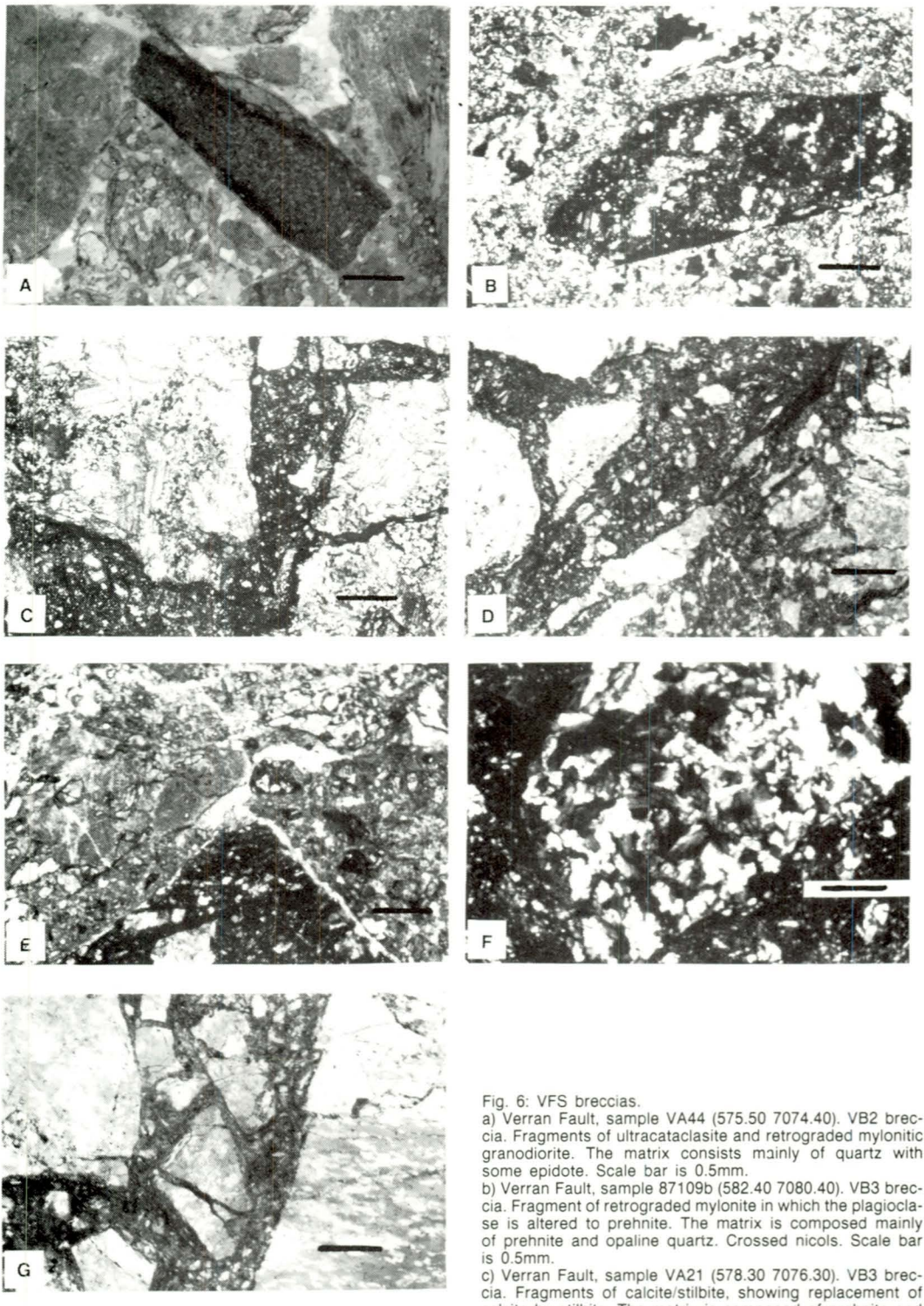

Fig. 6: VFS breccias.
a) Verran Fault, sample VA44 (575.50 7074.40). VB2 breccia. Fragments of ultracataclasite and retrograded mylonitic granodiorite. The matrix consists mainly of quartz with some epidote. Scale bar is 0.5mm.
b) Verran Fault, sample 87109b (582.40 7080.40). VB3 breccia. Fragment of retrograded mylonite in which the plagioclase is altered to prehnite. The matrix is composed mainly of prehnite and opaline quartz. Crossed nicols. Scale bar is 0.5mm.
c) Verran Fault, sample VA21 (578.30 7076.30). VB3 breccia. Fragments of calcite/stilbite, showing replacement of calcite by stilbite. The matrix is composed of prehnite and quartz. Scale bar is 0.5mm.
d) Verran Fault, sample 87109c (582.40 7080.40). VB3 brec-

pinch and swell and sometimes carry abundant sharp fragments; in other places they are mostly dominated by the prehnite-quartz matrix (Figs. 6b-d).

The Verran mylonites, crush breccias and cataclasites are cut by numerous, irregular, stilbite veins (Z2), and more rarely by calcite and laumontite veins (Z1). The stilbite-mineralised veins, in general, cut through the other mineralised veins. Thicker stilbite veins sometimes contain angular, rotated fragments of mylonite and could thus be classified as breccias. Faulting took place along the VFS roughly coevally with stilbite deposition, as shown by Figs. 8a and b, as well as later on (Fig. 8c). Along the Skurven fault (Fig. 4a), features ascribed to several phases of brittle deformation are shown in Fig. 8d.

Several phases of late, distributed, cataclastic crushing (Sibson 1986), such as microfaulting and microcracking, can be identified over wide areas, leaving large tracts of incohesive rubble. Surprisingly, the small-scale pattern of fractures along the Verran Fault principal displacement zone seems to mimic the pattern defined by the TM- and airphoto-lineaments in this area, but with an additional overprinted NW peak (Fig.3-*4*).

The Rautingdal fault

The sigmoidal Rautingdal fault (Fig. 4a), trending NNE-SSW at a high angle to the Verran Fault, provides spectacular outcrops of the cataclasite series rocks (Sibson 1977) as well as late zeolite mineralisation. The entire bottom of this narrow and steep-sided valley is made up of an approximately 10m wide, greenish cataclastic fault rock. Just outside the actual fault zone, arrays of en échelon gash veins are well preserved (Fig.9). The cataclasite (RB1), similar to VB1 along the Verran Fault, commonly consists of subrounded to subangular, medium-sized fragments of albitised plagioclase and secondary epidote in a fine-grained matrix of epidote, albite and K-feldspar (Figs.5a-c). Prehnite, chlorite and calcite also occur as matrix minerals. Calcite is also a common vein mineral. Parts of this cataclasite are transected by thin ultracataclasite stringers showing a very fine-grained, aphanitic groundmass. In places, the cataclasite shows a distinct red coloration which is caused by numerous haematite blebs and veinlets.

Along the actual slickensided fault plane, here indicating dip-slip movement, there is a 0.5-2 m wide ultracataclasite (RB2) (Figs. 7a-d). Widely dispersed angular fragments of retrograded mylonite, quartz, epidote and ultracataclasite occur. Some ultracataclasite fragments show evidence of three episodes of fragmentation. The minerals of the almost opaque, ultra-fine-grained matrix are difficult to determine optically, but XRD analysis shows that they consist mainly of quartz and laumontite. Close to the fault plane, up to 10 cm away, the ultracataclasite is transected by a laumontite-matrixed breccia (Figs. 7c & d). Both this and the ultracataclasite are dissected by a late network of hair-thin laumontite veinlets (Figs. 7a & d). The RB1 cataclasite is also cut by numerous 1-3 cm wide stilbite and calcite veins which trend ENE-WSW, i.e. parallel to the Verran Fault.

Just north of the Rautingdal fault, tunnels of the Ormsetfoss hydroelectric scheme expose numerous 10-30 cm wide gash veins filled with calcite and stilbite (Fig. 10). In addition, the granodioritic rock is usually 'rotten'; that is, altered to clay minerals over a width of approximately 2 m adjacent to these veins. Most veins trend NNE-SSW (Fig.3-*11*), i.e. parallel to the Rautingdal fault and to most of the prehnite-matrix breccias.

The Elvdal fault

This slightly curved fault trends ENE-WSW, subparallel to the main Verran Fault (Fig.4a), and displays fault rocks of a distinct upper crustal affinity. The actual fault zone is marked by brick-red breccias (EB1) and abundant stilbite (Z2) veining which also contribute to the distinct red coloration of the entire valley floor. The stilbite veins trend ENE-WSW, parallel to the trend of the actual fault.

The matrix-supported brick-red breccias

---

cia. Fragment of retrograded mylonite in fine-grained prehnite-quartz matrix. Scale bar is 0.5mm.

e) Elvdal Fault, sample VA34 (569.35 7071.35). EB1 breccia. Composite fragment consisting of ultracataclasite/pseudotachylyte (?) and retrograded mylonite, together with other fragments of mylonite in a zeolite matrix. Scale bar is 0.5mm.

f) Elvdal Fault, sample VA34 (569.35 7071.35). EB1 breccia. Fragment of vein stilbite and smaller fragments of milled down mylonite in a fine-grained zeolite matrix. Scale bar is 0.5mm.

g) Elvdal Fault, sample E1-87 (569.20 7071.20). EB1 breccia. Fragments of strained vein quartz in a zeolite matrix. Scale bar is 0.5mm.

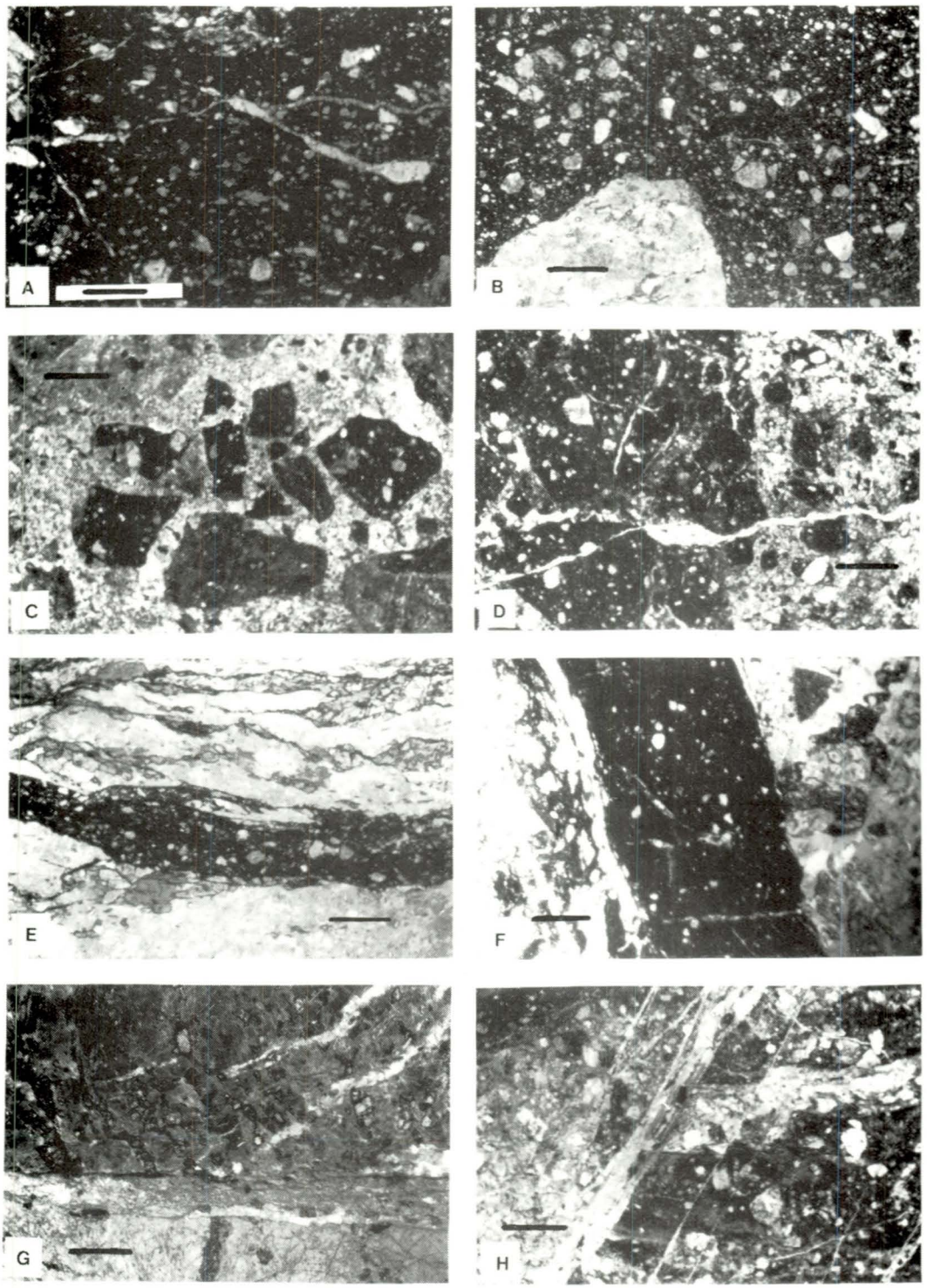
A
B
C
D
E
F
G
H

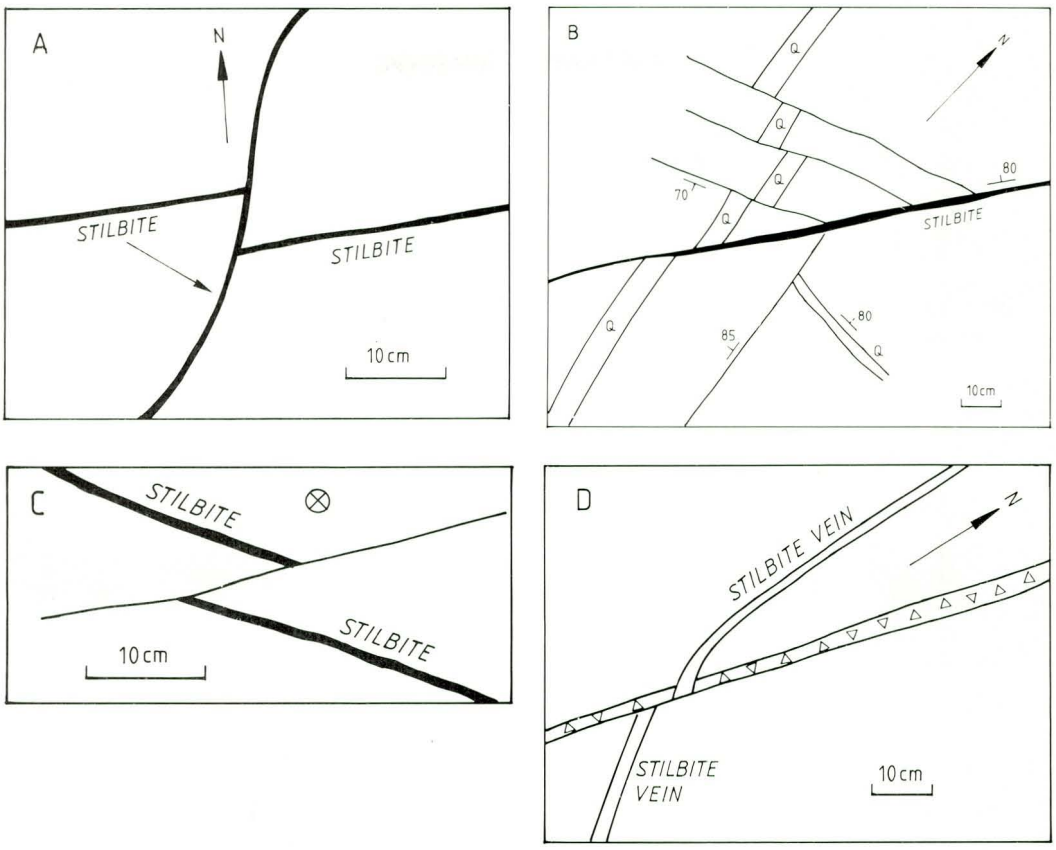

Fig. 8: Small-scale stilbite-mineralised faults and joints along the VFS.
a) Verran Fault (582.30 7080.20). Stilbite-mineralised vein transecting retrograde mylonite transected by late, stilbite-mineralised fault.
b) Verran Fault (579.90 7077.65). Early quartz-vein transecting retrograde mylonite cut by main stilbite-mineralised fault and non-mineralised splays from this.
c) Verran Fault (579.80 7077.65). Stilbite-mineralised vein transected by late, nearly horizontal fault.
d) Skurven fault (568.20 7080.20). Stilbite-mineralised vein transecting prehnite-matrix breccia. Evidence of late, post-stilbite deposition, fault movement along prehnite-matrix breccia trend.

Fig. 7: VFS ultracataclasites and vein mineralisations.
a) Rautingdal fault, sample 89-857-1 (579.20 7077.70). RB2 ultracataclasite. Fragments of albite, epidote and retrograded mylonite in an opaque groundmass, transected by late laumontite veins. Scale bar is 0.5mm.
b) Rautingdal fault, sample R-10 (579.20 7077.70). RB2 ultracataclasite. Somewhat rounded fragments of retrograde mylonite, albite and epidote in an opaque groundmass. Scale bar is 0.5mm.
c) Rautingdal fault, sample 89-857-3 (579.20 7077.70). Laumontite matrix breccia containing angular fragments of RB2 ultracataclasite. Scale bar is 0.5mm.
d) Rautingdal fault, sample 89-857-2 (579.20 7077.70). RB2 ultracataclasite. Ultracataclasite (left) cut by laumontite-matrixed breccia, and a younger thin laumontite vein. Scale bar is 0.5mm.
e) Hitra-Snåsa Fault, sample AG177 (565.00 7080.15). Pseudotachylyte paralleling the foliation of a mylonitic granodiorite. Scale bar is 0.5mm.
f) Hitra-Snåsa Fault, sample VA60 (577.10 7086.90). Pseudotachylyte vein transecting an early fault breccia. Scale bar is 0.5mm.
g) Sætervatn Fault, sample 87100 (581.70 7081.95). Stilbite-mineralised fault transecting mylonitic granodiorite. Scale bar is 0.5mm.
h) Verran Fault, sample VA31 (580.20 7077.90). VB1 cataclasite, with quartz vein, cut by a late vein of zeolite. Scale bar is 0.5 mm.

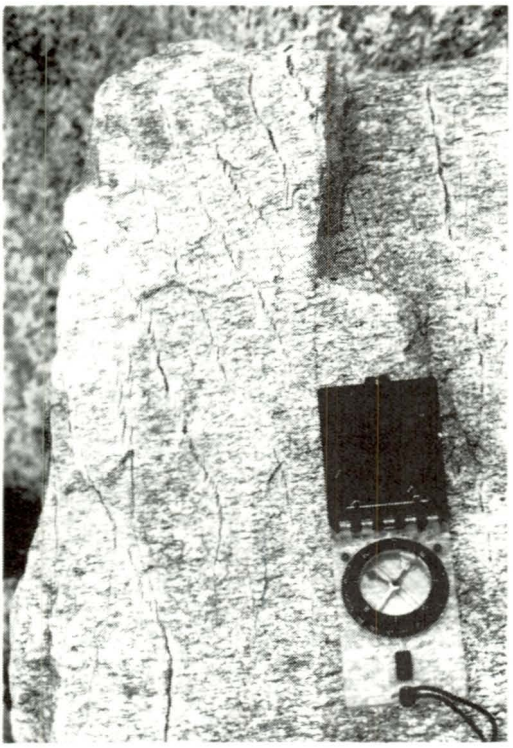

Fig. 9: Rautingdal, small-scale, en échelon gash veins in unaltered granodioritic gneiss.

contain coarse to medium-sized angular fragments which are composed mainly of retrograded mylonite (originally granodiorite), strongly undulose fragments of vein quartz (Fig. 6g), vein stilbite (Fig. 6f) and vein epidote. The plagioclase of the retrograded mylonite sometimes shows alteration to prehnite. Some of the fragments are composite and show evidence of three episodes of brecciation; and fragments of ultracataclasite/pseudotachylyte are also present (Fig. 6e). The red matrix is extremely fine-grained but SEM images show that it consists mostly of stilbite with some minute fragments of epidote and adularia, as well as comminuted mylonite. The brick-red colour is caused by abundant haematite inclusions, in addition to the red stilbite and adularia.

As the Elvdal brick-red breccia (EB1) contains stilbite both as fragments and as part of the matrix, it is evident that it formed at a very late stage in the development of the MTFZ. It is, however, clear that the EB1 was generated in an already existing zone of weakness, as evidenced by the abundant fragments of retrograded mylonite and hydrothermal quartz.

Beitstadfjord fault and fracture pattern

As shown by Bøe & Bjerkli (1989) in their shallow-seismic survey, the fault system of the Beistadfjord basin mimics the onland MTFZ fault pattern (Fig. 1a). The meso-scale fault pattern, however, is more complicated.

North of Beitstadfjord plumose and fringe structures occur on late NW-SE to NNW-SSE trending joints. These structures are developed only in the fine-grained metasandstones of this area and do not occur elsewhere on Fosen.

Along the eastern shores of Beitstadfjord (Fig.1a) abundant meso-scale faults and joints occur in metasandstone and show evidence of multiple episodes of fracturing. Early E-W trending quartz veins (Fig. 11a) are transected by a set of N-S to NNW-SSE trending mesofaults and also by shear-zones showing conjugate fault sets (Fig. 11a). The N-S trending faults and joints are themselves cut by late NW-SE trending joints with transverse minor joints (Fig. 11b).

En échelon gash veins (Fig. 11c), in which the trend of the vein array is close to NS, are common. Some are sigmoidal (Fig. 11d) and filled with calcite. En échelon gash veins are useful in determining the sense of shear as the vein array is usually parallel to the direction of shear. These small shear-zones are mainly of local significance and formed in response to minor movements on mesofaults. The overall, small-scale fault pattern is extensional and can probably be linked to an early stage in the formation of the Beitstadfjord half-graben, although this is difficult to prove conclusively.

Discussion

The VFS crush breccias and cataclasites which overprint retrograded rocks of the mylonite series show abundant evidence of high crustal level cataclasis, fracturing and micro- and meso- faulting. The depth of formation of the Verran Fault (VB1) cataclasite is not well constrained. The new mineral assemblage of VB1, albite-chlorite-epidote-(prehnite-haematite), is intermediate between the sub-greenschist paragenesis pumpellyite-chlorite-actino-

lite and the greenschist assemblage clinozoisite-chlorite-actinolite. According to Kamineni et al. (1988), this mineral assemblage is stable between 2.5 and 3.5 kb at temperatures of 325-375°C. For a geothermal gradient of 35°C/km this implies a maximum depth of formation between 9 and 11 km (Fig. 12).

The mechanism of formation of the VB2 breccia was by attrition brecciation and probably some distributed crush brecciation (Sibson 1986). Some of the fragments containing pseudotachylyte testify to early episodes of dry, seismic slip (Sibson 1975). The VB2 breccia was primarily a porous and incohesive breccia and its secondary cohesion was achieved mostly by precipitation of hydrothermal quartz. Silica-rich fluids must have been mobilised along the fault trace, either coeval with or succeeding dip-slip movement, and were precipitated when encountering lower temperature and/or pressure. The quartz matrix sealed the fault for an unknown period of time until it was re-crushed and remineralised with abundant hair-thin epidote and quartz veinlets. The depth of formation for VB2 is poorly constrained. In general, such a breccia would develop at crustal depths between 4 and 13 km (Sibson 1977), in the elasto-frictional (EF) regime. The absence of any ductile deformation of the quartz matrix points to a formation in the middle part of this regime. The presence of a small number of vein prehnite fragments supports a depth of formation in the lower reaches of the prehnite-pumpellyite facies (Fig. 12).

Field relationships show that the prehnite-

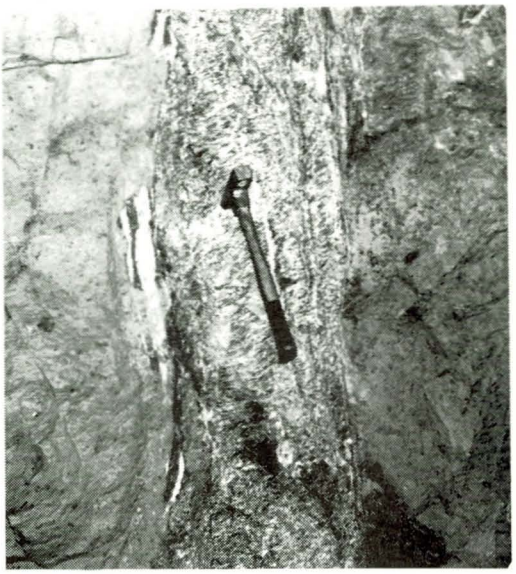

Fig.10: Ormsetfoss calcite-stilbite gash vein flanked by 'rotten', clay-altered, granodiorite. The hammer used as a scale is 30cm long.

matrix breccias (VB3) clearly formed at a later stage than VB1 and VB2. They transect the earlier breccias, mostly at a high angle, trending NNE-SSW. As prehnite constitutes a substantial part of the matrix and vein fill, this suggests a site of origin in the middle to upper parts of the EF regime. The general downward sequence of developed facies is zeolite → prehnite-pumpellyite → greenschist (Fig. 12). The zeolites and the prehnite-pumpellyite

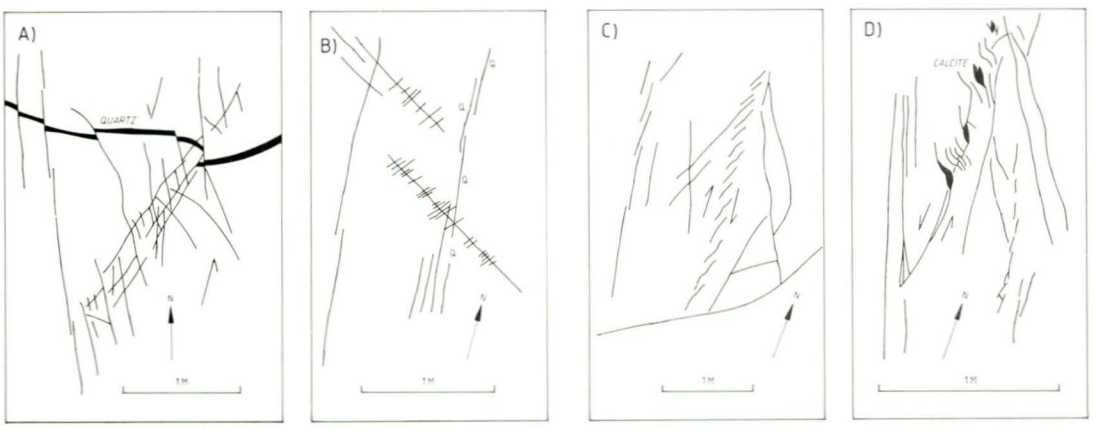

Fig. 11: Examples of mesoscale joint patterns from Beitstadfjord. See text for explanation.

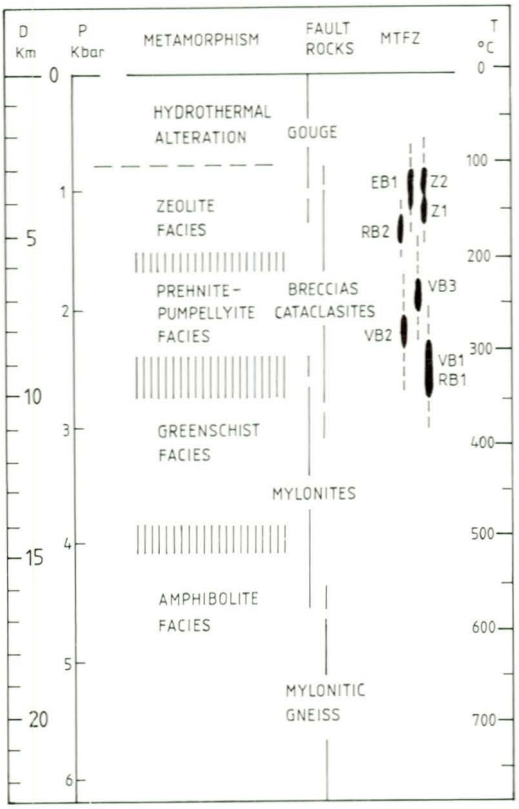

Fig. 12: Depth of formation of brittle fault rocks along the VFS. The figure has been adapted from Sibson (1983). The geothermal gradient in this particular case has been assumed to have been ca. 35°C/km.

facies minerals form by reaction of unstable initial minerals with fluids that pervade the fault system, within a certain range of pressure and temperature. The zeolites and prehnite were deposited in veins and originally incohesive breccias, probably by reaction between fluids and minerals such as plagioclase, quartz and calcite. Prehnite is stable up to 250-300°C, normally indicating crustal depths of 10 km or more, but considering the higher heat flow in a major fault zone the depth of formation in this particular case may have been considerably lower. Considering a geothermal gradient of 35°C/km, this would indicate a maximum depth of VB3 formation of 7-8.5 km (Fig. 12). The somewhat higher than normal geothermal gradient is reasonable since laboratory experiments and theoretical models (Turcotte et al. 1980, Sibson 1980) indicate that fault-zone temperatures are considerably elevated above those expected for the surrounding host rocks.

In the Miocene Tanzawa Mountains of Japan, there is a depth sequence consisting of stilbite (0-2 km)-laumontite (2-4 km)-prehnite (4-6 km) and albitised plagioclase (4-6 km) (Seki et al. 1969). However, in many cases there will be a considerable overlap of the different mineral phases, as shown by Liou (1971). Evidence from laumontite and stilbite veins along the Verran Fault, for example, shows that, in some cases, laumontite crystallised later than stilbite. Also, in the VFS, the laumontite and prehnite fields have overlapped in some cases, as evidenced by laumontite fragments in a prehnite matrix. According to Kristmannsdottir & Tomassen (1978), the temperatures at which stilbite and laumontite are stable are 70-170°C and 110-230°C, respectively.

The Rautingdal (RB1) cataclasite, which is very similar to the above-described VB1 cataclasite, would presumably, by the same line of argument, have formed at a maximum depth between 9 and 11 km (Fig. 12). The RB2 ultracataclasite, containing a significant proportion of laumontite, testifies to formation in an intermediate crustal position; as laumontite is one of the zeolites stable at highest temperatures, up to 230°C, i.e. a maximum depth of 6 km for a gradient of 35°C/km. This ultracataclasite thus probably formed later than the (VB3) prehnite-matrixed breccias occurring along the Verran Fault.

As stilbite is one of the zeolites which is stable at lowest temperatures (‹170°C), its widespread occurrence in veins along the entire VFS testifies to a major period of late-stage hydrothermal precipitation which was at least accompanied by some faulting activity (Fig. 8). At Ormsetfoss, stilbite and calcite occur together in gash veins. Stilbite is the major vein mineral along both the Verran Fault and the Elvdal fault. It was deposited in fractures of the upper crust, in connection with an episode of extensional fault activity. Along the Elvdal fault, the EB1 breccia contains fragments of vein stilbite, pointing to activity along this fault at a comparatively late stage.

With regard to the timing of faulting along the VFS, Oftedahl (1975) suggested that a major episode occurred in the Middle Jurassic, resulting in the downfaulting of the Beitstadfjord half-graben. Bøe & Bjerkli (1989) favoured Late Jurassic-Early Cretaceous fault-

ing, either dip-slip succeeded by dextral strike-slip, or oblique-slip in a transtensional regime. We suggest that this faulting activity broadly coincides with the major hydrothermal flux associated with stilbite deposition. Preliminary fission-track dating of apatite in a sample taken from the Verran Fault at Trongsundet (Fig. 4a), an area of intense stilbite mineralisation, gives an age of 144 ± 22 Ma (Grønlie et al., in prep.). As apatite has a closure temperature of 125 ± 25°C (Naeser 1981), this shows that the dated apatite cooled below this temperature at some time near the Jurassic/Cretaceous transition. Since this is the youngest apatite age of several from this region, the other samples from fresh country rocks showing Early Jurassic and Triassic cooling ages, it would appear that the Verran Fault was part of an active hydrothermal system during Jurassic times; and moreover, the hydrothermal system must have been associated with the post-Mid Jurassic downfaulting of the Beitstadfjord basin. The sample would then have been positioned at a depth of 3-4 km, corresponding to an average uplift/erosion of 0.02-0.03 mm/yr since Late Jurassic/Early Cretaceous time. The Elvdal fault would appear to have been active either at the same time as, or somewhat later than the Verran Fault.

Fission-track dating of zircon and sphene suggest that the study area had a tectonically complicated, early, pre-Jurassic history with complex fault block movements in Devonian and Permo-Triassic times (Grønlie et al., in prep.). The various VFS fault rocks, originating in different crustal depth positions, support this view. Palaeomagnetic dating of fault rocks has indicated Permian as well as Mesozoic hydrothermal activity and faulting, particularly in the area of inner Trondheimsfjord (Grønlie & Torsvik 1989). Fission-track dating indicates that the Triassic was a period of intense faulting and rapid uplift in the Trondheimsfjord area (Grønlie et al.,in prep.). Piasecki & Cliff (1988), in dating shear-zone pegmatites from Fosen, concluded that a major phase of orogen-parallel ductile shearing had taken place in the Middle Devonian at ca.389 Ma, probably coeval with a major episode of sinistral shear along the Hitra-Snåsa Fault (Grønlie & Roberts 1989). Most brittle fault rocks of the VFS can thus be assigned to the Late Devonian-Jurassic time span; the VB1/RB1 forming just above the brittle/ductile transition and possibly in Late Devonian times.

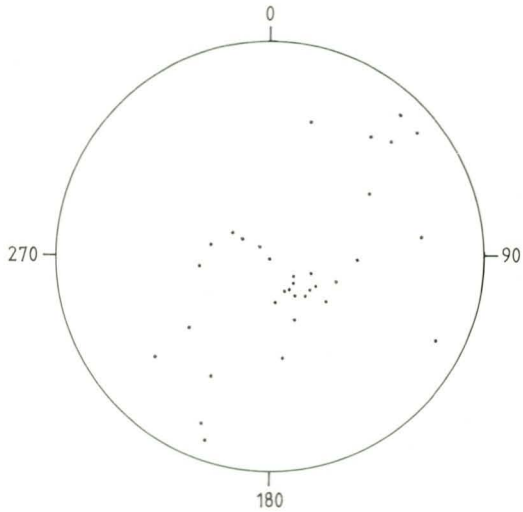

Fig. 13: Equal-angle projection (lower hemisphere) of slickenside lineations measured on individual, planar to curviplanar, anastomosing fault surfaces within the Verran Fault zone at Trongsundet (cf. Fig. 4a) (582.50 7080.70 - 580.50 7078.40).

It has earlier been postulated (Grønlie & Roberts 1989) that the VFS acted as a major, dextral, strike-slip fault-zone and defined a strike-slip duplex system (Woodcock & Fischer 1986) in Mesozoic times. This hypothesis, which was based mainly on a detailed Landsat TM lineament study (Rindstad & Grønlie 1986) and minimal field control, has not been conclusively proven even though the geometric configuration favours this interpretation. On account of the comparatively homogeneous gneissic lithologies, the question cannot be settled simply by bedrock mapping. Most late, minor brittle structures seen in the field are extensional in character. On the basis of slickenside data from late, minor faults, many of which are stilbite mineralised, Bering (1990) showed that σ_1 was oriented vertically along most of the MTFZ, thus favouring dip-slip normal fault movement. Along the Verran Fault zone on the north shore of Verrasundet, however, slickenside lineations vary considerably in plunge, from fault surface to fault surface, from near-vertical to near-horizontal (Fig. 13). The precise dating of fault movements is crucial here. It may be that a post-Z2 (post-Mid Jurassic) component of faulting was largely dip-slip or oblique-slip. Right-lateral movement could then have been either Late Jurassic/ Early Cretaceous or even Late Cretaceous/

Early Tertiary, at a time when reactivation is known to have occurred within the MTFZ (Grønlie et al. 1990). Whatever the case, it has been shown from seismic reflection profiling across southern Fosen that both the Verran and the Hitra-Snåsa Faults dip steeply and regularly to the northwest, penetrating to depths of 18-20km (Hurich & Roberts, in prep.). Their existence as major strike-slip faults thus appears indubitable.

Accepting the importance of dip-slip in the evolution of the VFS, the Verran and Elvdal faults could possibly be inferred as elements of an extensional fault system, with the high-angle Rautingdal fault functioning as a transfer fault (Bering 1990) (Figs.1a and 4a). However, the laumontite veining of the RB2 ultracataclasite indicates that the Rautingdal Fault was active prior to the main, probably Jurassic, stilbite (Z2) hydrothermal flux along the Verran and Elvdal Faults; but as the fields of laumontite and stilbite partly overlap, this is not conclusive.

On the basis of shallow seismic reflection evidence from the Beitstadfjord basin, Bøe & Bjerkli (1989) considered two genetically related models; one where Late Jurassic-Early Cretaceous dip-slip normal faulting was followed by dextral strike-slip movement; and another in which the deformation was by Late Jurassic oblique-slip and transtension. The first model would be in agreement with Grønlie & Roberts' (1989) interpretation, as well as with offshore observations and deductions (e.g. Larsen 1987).

The very latest stage of brittle fracturing on Fosen is represented by a set of NW-SE to NNW-SSE trending minor joints, in places showing plumose and fringe structures. It is uncertain how this set of clearly late small-scale joints relates to the pattern of master joints of the NW-SE trend seen in Outer Fosen. The general lack of fault rocks along the master joints indicates a rather simple tectonic history, as compared with the resurgent fault tectonism along the MTFZ. It is thus possible that the master joints reflect a regional stress pattern related to a specific episode in Earth history.

The geometric configuration of the master joints indicates that most fractures are confined to the shallow upper crust (Nur 1982, Gudmundsson 1987). This is no proof of a young age of initiation, however, as they could have been initiated at deeper levels in the crust, e.g. due to the influence of high cleft-water pressures which counteract the overburden effect and permit deep tensile fracture (Secor 1965). In gently folded platform areas, joints can show a well defined relationship to folds developed during the same tectonic event (Price 1966). On Fosen, the master joints are clearly not related to the two earliest phases of tight to isoclinal folding which produced lunate and arrowhead fold interference patterns (Roberts 1986). They could, however, possibly be interpreted as 'ac' joints (Price 1966) relating to the latest, NE-SW trending, gentle to open folds of Late Devonian (Svalbardian/Solundian) age. The joint and fault pattern observed in the Ørlandet ORS by Siedlecka (1975) is indeed in accordance with such an interpretation. Siedlecka (1975), furthermore, suggested that Tertiary tectonic events may have reactivated existing fractures of this trend, but also created new joints and faults. If the fractures are of Devonian age they show a surprising lack of fault rock products; and the question arises as to why they were not reactivated at some stage during the Mesozoic as in the case of faults along the MTFZ.

Offshore, in addition to the three main Mesozoic fault trends (N-S, NE-SW and ENE-WSW), Gabrielsen et al.(1984) recognised a fourth (NW-SE) trend which resulted from Tertiary tectonic activity or possibly from a reactivation of older structures. Seismic profiling in the Mesozoic Edøyfjord basin, just southwest of the study area, by Bøe & Bjerkli (1989) also showed several faults of the same trend. It is thus reasonable to assume that many of the on-land, NW-SE trending, master joints and faults were initiated in Late Mesozoic or Tertiary times.

The widespread occurrence of fractures of this trend could be interpreted as having been caused by a stress field generated by ridge push and associated lithospheric drag forces, subsequent to the Palaeocene/Eocene opening of the Norwegian-Greenland Sea, and such a model is depicted in Fig. 14. As first maintained by Husebye et al.(1978), the opening of the Norwegian-Greenland Sea is likely to have produced ridge-push related forces creating compressive stresses within the plates on either side of the mid-oceanic ridge. Stephansson (1988) also concluded that the ridge-spreading stress created at the Mid-Atlantic ridge is the main contributor to the current stress field in Fennoscandia. In general, it has been found

that much of continental Europe, the North Sea area and the British Isles shows a consistent NW-SE trend of the maximum horizontal stress (Klein & Barr 1986).

In situ stress measurements have been carried out at Ormsetfoss, near Verrabotn, by Hanssen & Hansen (1987) employing the overcoring technique. These show that σ_1 is nearly horizontal and oriented E-W. The local stress situation is thus considerably influenced by topographically induced stresses and tectonic residual stresses. As expected, there is no apparent correlation between the present rock stress situation in this area and the trends of major fractures (Fig.1a). In contrast, in situ stress measurements from the Fosdalen mine at Malm, 40km to the east, shows σ_1 to be oriented close to N-S. At present, no in situ stress measurements have been reported from the Outer Fosen area.

Recent earthquake activity in Norway has been centred in the offshore Meløy and Ålesund regions. The Møre-Trøndelag area is also a region of considerable seismic activity. Important faults in Central Norway that are seismically active today, at least along specific segments, include the MTFZ, the Kristiansund-Bodø Fault Complex and the Rana Fault Complex (Bungum 1989, Bungum et al. 1991). From Scandinavian earthquakes as a whole, Bungum et al. (1991) have shown that the inferred maximum stress orientations approximate to a NW-SE trend. These same authors found that fault plane solutions from southeastern Norway are the ones that correspond closest to the NW-SE ridge push direction. Along the continental margin, however, conditions are more complex and require consideration of other sources of stress in addition to that caused by plate movements. One possible stress generating mechanism is that of lithospheric loading/unloading due to sedimentation and/or glaciation. In Tertiary times, the study area was affected by numerous episodes of uplift and sedimentation. Rundberg (1989) distinguished between five major phases of uplift prior to the Pleistocene in the northern North Sea. The first, Palaeocene uplift was probably of a flexural style, while the subsequent phases of uplift to a large degree reactivated the pre-existing basin margin faults. A particularly strong uplift occurred in Pliocene times, as indicated by the deposition of more than 1000 m of prograding Pliocene sediments in the Haltenbanken area (Rundberg 1989).

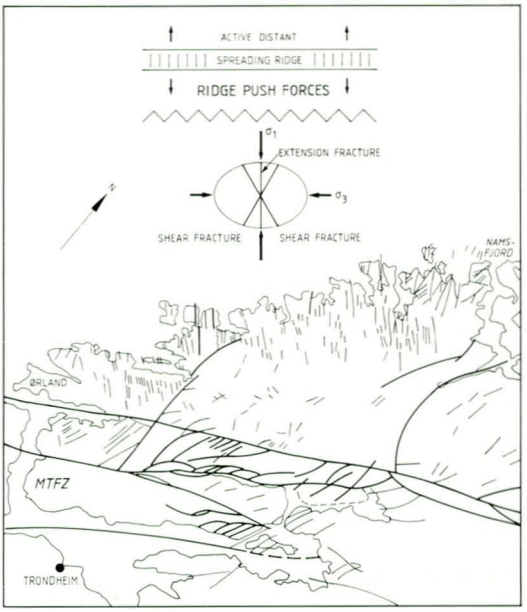

Fig. 14: Possible ridge-push initiation of the NW-SE trending master joints and faults in the Outer Fosen area (see text for discussion). Adapted from Olsen (1987).

The postglacial uplift of Fennoscandia is another source of stress accumulation which has resulted in neotectonic activity in northern Scandinavia (Lundquist & Lagerbäck 1976, Olesen 1988). At present, there is no evidence of recent fault activity in the study area, such as that documented from southwest Norway (Anundsen 1989). Bungum et al. (1991) do, however, maintain that the dominant source of stress, also in the coastal margin area, is the ridge-push effect from plate movements.

Conclusions

The post-Caledonian deformation of rock units occurring along the VFS represents a time sequence where lower crustal ductile deformation was followed by several episodes of brittle fragmentation. The main stages of development are as follows.

(1) On the basis of evidence from various kinematic indicators we maintain that the Verran Fault was subject to one or more episodes of ductile sinistral shear in Late Silurian to Middle Devonian times.

(2) This was followed by retrogression of the

mylonites and granodioritic rocks within and close to the principal displacement zone.
(3) Several later episodes of brittle faulting followed, some of which were accompanied by major pulses of hydrothermal fluids. We conclude that major, brittle faulting events took place in Late Devonian, Permo-Triassic and post-Mid Jurassic times. As indicated by apatite fission-track data, the major phase of hydrothermal activity and zeolite mineralisation is associated with the post-Mid Jurassic downfaulting of the Beitstadfjord half-graben. Apatite from the Verran Fault cooled below the blocking temperature of apatite (125 ± 25°C) approximately at the boundary between the Jurassic and Cretaceous periods (144 ± 22 Ma). Most brittle fault rocks along the MTFZ in this region were formed in the time interval from Late Devonian to Jurassic.
(4) Although brittle fault rocks and other minor structures along the MTFZ do not directly favour any *major* lateral displacements in Mesozoic time, the general geometric configuration points to significant dextral strike-slip. Ongoing seismic reflection work also indicates that the major faults in the MTFZ are deep-seated strike-slip structures. The model proposed by Bøe & Bjerkli (1989) in which a Late Jurassic/ Early Cretaceous phase of dip-slip normal faulting was followed by a phase of dextral strike-slip faulting is favoured.
(5) It is postulated that most of the NW-SE trending faults and master joints on Outer Fosen are related to Tertiary tectonic events and most likely caused by a stress field created by ridge-push generated from the Mid-Atlantic spreading ridge.
(6) The latest stage of brittle fracturing on Fosen is represented by a set of NW-SE to NNW-SSE trending minor joints, in places showing plumose and fringe structures. It is uncertain how these small-scale joints relate to the pattern of master joints and faults of the same trend on Outer Fosen, but it is possible that they were initiated in postglacial times.

Acknowledgements
The authors are grateful to Roy Gabrielsen, Asbjørn Thon, Geoff Milnes and Joe Hull for their helpful comments on an early version of the manuscript. This led to a major revision, and to an expansion of the discussion of certain topics. Stephen Lippard and Reidulv Bøe reviewed the revised manuscript at quite short notice and suggested further small alterations. Gunnar Grønli and Ingemar Aamo of the NGU staff are thanked for their participation in drafting and photography.

References

Aanstad, K.M., Gabrielsen, R.H., Hagevang, T. Ramberg, I.B. & Torvanger, O. 1981: Correlation of offshore and onshore structural features between 62°N and 68°N, Norway. *Proc. Norw. Symp. on Exploration, Bergen 11,* 1-25.

Anundsen, K. 1989: Late Weichselian relative sea levels in southeast Norway: observed strandline tilts and neotectonic activity. *Nor.Geogr.Tidsskr. 111,* 288-292.

Bering, D.1990: Paleostress i deler av Møre-Trøndelag forkastningssone. *Geonytt 1/90,* 28.

Bevan, T.G. & Hancock, P.L. 1986: A late Cenozoic regional mesofracture system in southern England and northern France. *J.Geol.Soc.London 143,* 355-362.

Bucovics, C., Cartier, E.G., Shaw, N.D. & Ziegler, P.A. 1984: Structure and development of the mid-Norway continental margin. *Petroleum Geology of the North European Margin,* 407-423.

Bungum, H. 1989: Earthquake occurrence and seismotectonics in Norway and surrounding areas. *In* Gregersen, S. & Basham, P.W.(eds.): *Earthquakes at North-Atlantic Passive Margins: Neotectonics and Postglacial Rebound.* Kluwer Academic Publishers, 501-519.

Bungum, H., Alsaker, A., Kvamme, L.B. & Hansen, R.A. 1991: Seismicity and seismotectonics of Norway and nearby continental shelf areas. *J.Geophys.Res.96,* 2249-2265.

Bøe, R. & Bjerkli, K. 1989: Mesozoic sedimentary rocks in Edøyfjorden and Beitstadfjorden, Central Norway: implications for the structural history of the Møre-Trøndelag fault zone. *Mar.Geol.8700,* 287-299.

Bøe, R. & Sturt, B.A. 1991: Textural responses to evolving mass-flows: an example from the Devonian Asen Formation, central Norway. *Geol.Mag.128,* 99-109.

Fossen, H., Bank, H. & Möller, C. 1988: Roan berggrunnskart 1623-3, 1:50.000. Foreløpig utgave. *Nor.geol. unders.*

Gabrielsen, R.H. & Ramberg, I.B. 1979a: Fracture patterns in Norway from Landsat imagery: results and potential use. *Proceedings of the Norwegian Sea Symposium, Tromsø, Norwegian Petroleum Society, NSS 23,* 1-28.

Gabrielsen, R.H. & Ramberg, I.B. 1979b: *Fracture maps Møre-Trøndelag region. Tectonic analysis of satellite imagery.* Unpubl. report, Dept. of Geology, Univ.of Oslo, 32pp.

Gabrielsen, R.H., Færseth, R., Hamar, G. & Rønnevik, H. 1984: Nomenclature of the main structural features of the Norwegian Continental Shelf north of the 62nd parallel. *Petroleum Geology of the North European Margin,* 41-60.

Gee, D.G ., Guezou, J.C., Roberts, D. & Wolff, F.C. 1985: The central-southern part of the Scandinavian Caledonides. *In* Gee, D.G. & Sturt, B.A.(eds.): *The Caledonide Orogen-Scandinavia and Related Areas.* John Wiley & Sons, Chichester, 109-133.

Grønlie, A. & Möller, C. 1988: Stokksund berggrunnskart 1523-2, 1:50.000. Foreløpig utgave. *Nor.geol.unders.*

Grønlie, A. & Roberts, D. 1989: Resurgent strike-slip duplex development along the Hitra-Snåsa and Verran Faults, Møre-Trøndelag Fault Zone, Central Norway. *J.Struct.Geol.11,* 295-305.

Grønlie, A., Harder, V. & Roberts, D. 1990: Preliminary fission-track ages of fluorite mineralisation along fracture zones, inner Trondheimsfjord, Central Norway. *Nor. Geol. Tidsskr. 70,* 173-178.

Gudmundsson, A. 1987: Tectonics of the Thingvellir fissure swarm, SW Iceland. *J.Struct.Geol.9,* 61-69.

Hanssen, T.H. & Hansen, S.E. 1987: Bergspenningsmåling i Ormsetfoss Kraftstasjon. *SINTEF rapport STF36 F87104,* 9pp.

Horn, G. 1931: Über Kohlengerölle in Norwegen. *Nor. Geol. Tidsskr. 12,* 341-361.

Husebye, E.S., Bungum, H., Fyen, J. & Gjøystdal, H. 1978: Earthquake activity in Fennoscandia between 1497 and 1975 and intraplate tectonics. *Nor.Geol.Tidsskr.58,* 51-68.

Kamineni, D.C., Thivierge, R.H. & Stone, D. 1988: Development of a cataclastic fault zone in an Archean granitic pluton of the Superior province: Structural, geochemical, and geophysical characteristics. *Am.J.Sci.288,* 458-494.

Klein, R.J. & Barr, M.V. 1986: Regional state of stress in Western Europe. *Proceedings of the International Symposium on Rock Stress and Rock Stress Measurements 4, Stockholm 1-3 September 1986,* 33-44.

Kristmannsdottir, H. & Tomassen, J. 1978: Occurrence, properties, use: *In* Sand, L.B. & Mumton, F.A.(eds) *Natural zeolites.* Pergamon Press, Oxford.

Larsen, V. 1987: Tectonic related stratigraphy in the north in the North Atlantic region from Bathonian to Cenomanian time. *Nor.Geol.Tidsskr.67,* 281-293.

Liou, J.G. 1971: P-T Stabilities of Laumontite, Wairakite, Lawsonite, and Related Minerals in the System $CaAl_2Si_2O_8$-SiO_2-H_2O. *J.Petrology 12,* 379-411.

Lundquist, J. & Lagerbäck, R. 1976: The Pärve Fault: A late glacial fault in the Precambrian of Swedish Lapland. *Geol.För.Stockholm Förh.98,* 45-51.

Naeser, C.W. 1981: The fading of fission-tracks in the geological environment data from deep drill holes. *Nuclear Tracks 5,* 248-250.

Nur, A. 1982: The origin of tensile fracture lineaments. *J. Struct.Geol.4,* 31-40.

Oftedahl, C. 1975: Middle Jurassic graben tectonics in mid Norway. *Proceedings Jurassic Northern North Sea Symposium 21,* 1-13.

Olesen, O. 1988: The Stuoragurra Fault, evidence of neotectonics in the Precambrian of Finnmark, northern Norway. *Nor.Geol.Tidsskr.68,* 107-118.

Olsen, J.C. 1987: Tectonic evolution of the North Sea Region. *In* Brooks, J. & Glennie, K.(eds.) *Petroleum Geology of North West Europe,* Graham & Trotman, 389-401.

Piasecki, M.A.J. & Cliff, R.A. 1988: Rb-Sr dating of strain-induced mineral growth in two ductile shear zones in the Western Gneiss Region of Nord-Trøndelag, Central Norway. *Nor.geol.unders.413,* 33-50.

Price, N.J. 1966: *Fault and Joint Development in brittle and semi-brittle rock.* Pergamon Press, 176 pp.

Reite, A.J. 1987: Rissa. Quaternary geological map M711 1522-2, scale 1:50.000, with description (in Norwegian). *Nor.geol.unders.skr.82,* 1-22.

Rindstad, B.I. & Grønlie, A. 1986: Landsat TM-data used in the mapping of large-scale geological structures in coastal areas of Trøndelag, Central Norway. *Proceedings of a Workshop on Earthnet Pilot Project on Landsat Thematic Mapper Applications, Frascati, Italy, December 1987,* 169-181.

Roberts, D. 1986: Structural photogeological and general features of the Fosen-Namsos Western Gneiss Region of Central Norway. *Nor. geol. unders. Bull. 407,* 13-25.

Rundberg, Y. 1989: *Tertiary sedimentary history and basin evolution of the Norwegian northern North Sea between 60-62°N; an integrated approach.* Unpubl.Dr.ing.thesis, Norwegian Institute of Technology, University of Trondheim.

Secor, D.T. 1965: Role of fluid pressure in jointing. *Am.J. Sci.263,* 633-646.

Seki, Y., Oki, Y., Matsuda, T., Mikami, K. & Okumura, K. 1969: Metamorphism in the Tanzawa Mountains, Central Japan. *J. Japan Assoc. Miner. 61,* 1-75.

Sibson, R.H. 1975: Generation of Pseudotachylyte by Ancient Seismic Faulting. *Geoph.J.Royal Astr.Soc.43,* 775-794.

Sibson, R.H., Moore, J.McM., Rankin, A.H. 1975: Seismic pumping - a hydrothermal transport mechanism. *J.Geol. Soc.London 131,* 653-659.

Sibson, R.H. 1977: Fault rocks and fault mechanisms. *J. Geol.Soc.London 133,* 191-214.

Sibson, R.H. 1980: Power dissipation and stress levels on faults in the upper crust. *J.Geoph.Res.85,* 6239-6247.

Sibson, R.H. 1983: Continental fault structure and the shallow earthquake source. *J.Geol.Soc.London 140,* 741-767.

Sibson, R.H. 1986: Brecciation processes in fault zones: Inferences from earthquake rupturing. *PAGEOPH 124,* 159-175.

Sibson, R.H. 1987: Earthquake rupturing as a mineralizing agent in hydrothermal systems. *Geology 15,* 701-704.

Siedlecka, A . 1975: Old Red Sandstone lithostratigraphy and sedimentation of the Outer Fosen area, Trondheim region. *Nor.geol.unders.321,* 1-35.

Solli, A. 1990: Namsos 1:250.000, foreløpig berggrunnsgeologisk kart. *Nor.geol.unders.*

Stephansson, O. 1988: Ridge push and glacial rebound as rock stress generators in Fennoscandia. *Bull.Geol.Inst. Univ. Uppsala 14,* 39-48.

Thorsnes, T. & Grønlie, A. 1990: Åfjord berggrunnskart 1622-4, 1:50.000, foreløpig utgave. *Nor.geol.unders.*

Torske, T. 1983: A fluidization breccia in granite at Skaget, Svellingen, Frøya. *Nor.geol.unders.380,* 107-123.

Turcotte, D.L., Tag, P.H. & Cooper, R.F. 1980: A steady state model for the distribution of stress and temperature on the San Andreas Fault. *J.Geoph.Res.85,* 6224-6230.

Wolff, F.C. 1976: Geologisk kart over Norge, berggrunnskart Trondheim 1:250.000. *Nor.geol.unders.*

Woodcock, N.H. & Fischer, M. 1986: Strike-slip duplexes. *J.Struct. Geol.8,* 725-735.

Original m/s received January 1990; revised and final m/s accepted June 1991.